22.5
Mini-D_2
A source for ultracold neutrons at FRM-II

I. Altarev[1], F.J. Hartmann[1], S. Paul[1], W. Schott[1], U. Trinks[1]
K. Gobrecht[2], E. Gutsmiedl[2], A. Scheuer[3]

1:Physik-Department E18, Technische Universität München D 85748 Garching
2:FRM-II , Technische Universität München D85748 Garching
3:TÜV Rheinland, D51105 Köln

Summary

The new Munich high-flux reactor FRM-II offers the possibility to install a unique source for ultracold neutrons (UCN), the Mini-D_2 UCN source, with a small volume of solid deuterium at a temperature of 5 K as converter, exposed to the cold neutron flux. This new source, being dedicated for storage experiments, is designed to be much superior to any existing UCN facility.

In the pulsed operation mode the Mini-D_2 source is expected to provide UCN densities up to 10^4 n/cm^3. This density is orders of magnitude larger than that from the best existing source at Institut Laue Langevin (ILL) in Grenoble (~50 n/cm^3 at the exit of the neutron turbine).

The large gain factor will enable new precision measurements of elementary properties of the free neutron, especially the electric dipole moment, the lifetime, and the angular correlation coefficients of the decay. These quantities are of fundamental interest in particle physics.

Operated in the continuous mode, the UCN source will provide an UCN flux density of up to $5 \cdot 10^5$ n/cm^{2}s at the exit, to be compared with ~$3 \cdot 10^4$ n/cm^{2}s at ILL. This improved UCN-flux offers new possibilities for traditional studies with UCN.

1. Introduction

Ultracold neutrons can be stored

Ultracold neutrons (UCN) have such low energies that they are reflected by many materials at all incident angles and can be stored in material bottles or confined by magnetic potential walls. For instance, the effective UCN potential of Beryllium is U_{Be}=252neV, equivalent to a height h in the earth's gravitational field respectively to a magnetic induction B, corresponding to a neutron velocity v, wavelength λ and temperature T of:

U_{Be} = 252 neV h = 257 cm B = 4.19 T v = 6.9 m/s λ = 57 nm T = 3 mK

Storage experiments superior

Long observation times

Relative measurements

Losses due to absorption or up-scattering can be as small as $5 \cdot 10^{-5}$ per wall collision for Be at a temperature < 30 K. Thus storage times of several minutes may be obtained, compared with observation times of milliseconds in typical beam experiments. Storage experiments make possible high- precision measurements of the properties of the free neutron and its decay, which are superior to any other method.

For instance, the extraordinary sensitivity in the detection of a possible electric dipole moment (EDM) of the neutron is directly related to the observation time. The present upper limit of the EDM is $d_n < 10^{-25}$ e·cm [Alt96], [Smi90].

In the case of the lifetime measurement in a storage experiment, no absolute calibration is needed, neither for the neutron flux nor for the effective volume, where decays may be observed, nor the detection efficiencies for the decay protons or electrons [Pau..], [Küg..]. The best present value for the lifetime is $\tau_n = 886.7 \pm 1.9$ s.

Key experiments:

EDM

n-lifetime

Asymmetry coefficients

These experiments as well as the measurements of the other decay parameters of the neutron are of great fundamental interest. The physics interest behind the EDM experiment is related to the observation of the breaking of a fundamental symmetry in particle physics (CP symmetry), which is reflected in the asymmetry of matter over antimatter in the universe. This symmetry breaking is not understood and belongs to the most exciting topics in particle physics, both theoretically and experimentally. A sensitivity increase in the determination of the neutron EDM (of which the pure existence would be another effect of CP-symmetry breaking) by 1-2 orders of magnitude could either establish or falsify the most popular super-theory of particle physics (super-symmetry). Currently two large accelerators are built to address just this question.

The neutron decay rate is proportional to $(g_V^2+3g_A^2)$, with g_V and g_A the weak vector and axial vector coupling constant. The value of g_A is only available from neutron decay. The neutron lifetime measurement together with other decay parameters tests the electro-weak Standard Model. However, at least equally important is the impact on other fields of physics, where the weak coupling constants are needed to calculate cross sections for applications, as in big bang cosmology, in astrophysics, in solar physics (e.g. for the solar neutrino problem), and in neutrino detection efficiencies.

2. The Munich concept of an UCN source

2.1 Basic ideas

The Mini-D_2 UCN source is foreseen to provide UCN densities of up to 10^4 n/cm^3 corresponding to a gain factor of ~200 compared to the source at ILL. To achieve this the concept of Mini-D_2 is based on three ideas:

Mini-D_2 : Super-thermal source

- The temperature of the converter for the production of UCN by down-scattering of faster neutrons is sufficiently low, so that the equilibrium of UCN production and losses will no longer be determined by up-scattering, but by absorption in the converter only (super-thermal source).
- At FRM II the UCN will be produced continuously. Storage experiments are to be refilled typically every few minutes. In order to match the continuous production operation to the pulsed filling requirements the UCN should be accumulated in the intermediate periods (storage source).
- Attention has to be paid to the transfer of UCN from the converter near to the centre of the reactor to the experimental area outside. The UCN density at the exit of the neutron turbine at ILL is ~50 n/cm^3. The initial densities finally obtained in the succeeding storage experiments some 5 m apart from the turbine exit are generally of the order of 1 n/cm^3. Almost two orders of magnitude are lost by transportation and mismatching. In Mini-D_2 the accumulating storage vessel is at the same time the UCN guide from near to the reactor core at the converter to outside of the biological shield at the entrance of the experiment in the experimental hall. In the ideal case the UCN density in the converter is transferred to the outside end of the accumulator tube with only minor losses. For this the accumulator has to be well designed with respect to volume, geometry and properties of the walls and windows.

The principle of the source is discussed in more detail in [Tri98, Tri00]. It is a development, which was inspired by a proposal of a thin film source [Gol83, Yu86], though the Mini-D_2 converter is a small block, not a film.

Previous work

First experimental work on a solid D_2 UCN source with rather big volume (6 liter) was performed in Gatchina [Alt80, Ser94, Ser95, Ser97]. Presently this source is not operating any more.

Other proposals

Recently UCN production in a solid ortho-D_2 converter (< 1 liter) exposed to premoderated spallation neutrons were studied at LANSCE, Los Alamos (see below) [Car00]. Based on these results a dedicated pulsed UCN source is proposed at LANSCE (~1.1 liter D_2 at ~ 5 K). In the storage bottle above the converter UCN densities of up to 400 n/cm^3 are expected.

Similar plans are under way at the neutron spallation source of PSI, Villigen.

At the moment both statistical and systematic errors are largely determined by the comparatively low UCN density: with the measuring times available at high-flux reactors they forbid not only accumulating a sufficient number of events but also hinder a very thorough test for systematic uncertainties. An increase of UCN densities by orders of magnitude would open a completely new range of accuracy.

Quasielastic UCN scattering for low momentum transfer

There are, in addition, interesting experiments on the more application-oriented side. UCN are very well suited to investigate the surfaces of solids and liquids. Here one of the most promising methods is quasi-elastic scattering at low energy transfer $\hbar\omega$ and low momentum transfer $\hbar\omega$. UCN and instruments like the gravity diffractometer [Ste92] or NESSIE [Ste83] with their very good energy resolution could extend the accessible energy-transfer range to values below a few neV, a region never reached before [Mic97]. Furthermore, the gap in momentum transfer between the $\hbar\omega$ values accessible by optical spectroscopy (below 0.005 $Å^{-1}$) and that exploitable with the neutron-spin-echo technique (above 0.015 $Å^{-1}$) could be closed. The measurements with UCN were always hampered by a profound lack in neutron flux. An increase by about one order of magnitude would change this situation considerably.

Reflectometry

The unprecedented resolution of gravity-based neutron-spectroscopy arrangements will also allow improvements in reflectometry studies. The determination of the critical energy is, e.g., a way to very precisely determine the scattering length of elements. Another application would be reflectivity measurements of thick films: the complicated fringe pattern generated could be resolved, and density measurements in layers up to a few μm below the surface could be performed. Among the interesting applications are investigations on protective layers for preventing oxidation of metals or corrosion problems.

In principle the investigation of magnetic surfaces is - due to the magnetic moment of the neutron - *the* domain for UCN. They are easily polarized, and their polarization – which is changed during interaction if the probe magnetization is not aligned with the neutron spin – is easily detected. Such measurements may be of interest for the technology of magnetic storage devices.

Tests of quantum mechanics

But UCN offer even more interesting possibilities. They reach from basic quantum-mechanics experiments like the detection of neutron bound states in box-like potentials in thin layers [Ste80] or even in the gravity potential of the earth to neutron microscopy [Arz86, Ste88]. All experiments would profit tremendously from the strongly increased flux to be expected at the new UCN source at FRM-II.

2.2 The converter

A super-thermal source

The general way to a source with high UCN intensity is to shift the maximum of the Maxwellian velocity distribution to values as low as possible by minimizing the moderator temperature. UCN are produced by down-scattering of higher-energy neutrons, i.e. neutrons which lose energy by creating phonon excitations in the moderator material. The UCN produced travel through the moderator scattering elastically, until they (a) escape from the moderator, (b) are captured or (c) up-scattered to leave the UCN-energy region. Up- and down-scattering are balanced at thermal equilibrium. The phonon spectrum in the moderator and thus the up-scattering depends strongly on the moderator temperature. Below a critical temperature, where the UCN-loss rate due to up-scattering is negligible compared to absorption, the equilibrium becomes independent of temperature. Below this temperature no gain in UCN yield can be achieved. The resulting source is called super-thermal.

Solid D_2 converter

The neutron moderator (hereafter called the converter) should have a high inelastic scattering cross section and low absorption cross section. A possible converter material is solid D_2, which combines rather low absorption cross section and high UCN conversion yield at a temperature of about 5 K. Figure 1 depicts calculations of UCN densities in solid D_2 as a function of its temperature [Sei99]. Following [Yu86] the calculations are based on phonon-energy spectra and density of states of solid and liquid ortho-deuterium, respectively. An incoming cold neutron flux of $\Phi_0 = 2.4 \cdot 10^{13}$ n/cm^{2}s was assumed with a Maxwellian energy spectrum corresponding to a temperature of $T_n = 40$ K. This is a realistic assumption for the location foreseen, in the nose of the beam-tube SR-4 at FRM II, which looks horizontally on the cold source. The curve shows, that the UCN density increases with decreasing temperature of the D_2, reaching a plateau for very low temperatures. At 5 K the UCN density is $\sim 1.3 \cdot 10^4$ n/cm^3. The UCN density in liquid D_2 at 19 K is also shown in Fig.1 for comparison. The gain factor in the UCN density for solid D_2 at 5 K as compared to liquid D_2 is about 60.

The temperature dependence of the UCN density in solid D_2 is mainly due to the temperature dependence of the up-scattering cross section, as shown in Fig.2 in combination with the temperature independent absorption cross section. Below a temperature of ~5 K up-scattering in solid deuterium is less important than absorption. Thus further cooling would result in minor improvements only. This result favors the convenient cooling with helium at a temperature just above 4.2 K.

D_2 temperature < 5 K

Incoming neutron flux $T_n \sim 30$ K

D_2 volume < 1 l

In Fig.3 the UCN density is shown as a function of the temperature T_n of the incoming neutron flux, for solid D_2 at 5 K, at 17 K, and for liquid D_2 respectively. For solid D_2 a flat maximum appears at $T_n \sim 30$ K. This fits well to the cold neutron flux from the liquid-D_2 cold source at FRM II, operated at ~25 K, resulting in an effective neutron temperature of $T_n \sim 40$ K.

The dimensions of the converter should be matched to the effective diffusion length of UCN in deuterium (~14 cm). The probability to escape from the converter is small for UCN from deeper layers. Therefore the volume of the D_2 may be less than ~ 1 liter. A small volume also is advantageous with respect to the heat load by neutron and γ radiation. The maximum temperature may be smaller, and with it the up-scattering.

Fig. 1

Maximum UCN density in ortho-D_2 for a cold neutron flux $\Phi(40K) \sim 2.4 \cdot 10^{13}$ n /cm^{2}s as a function of the D_2 temperature, as calculated from the phonon spectra in D_2

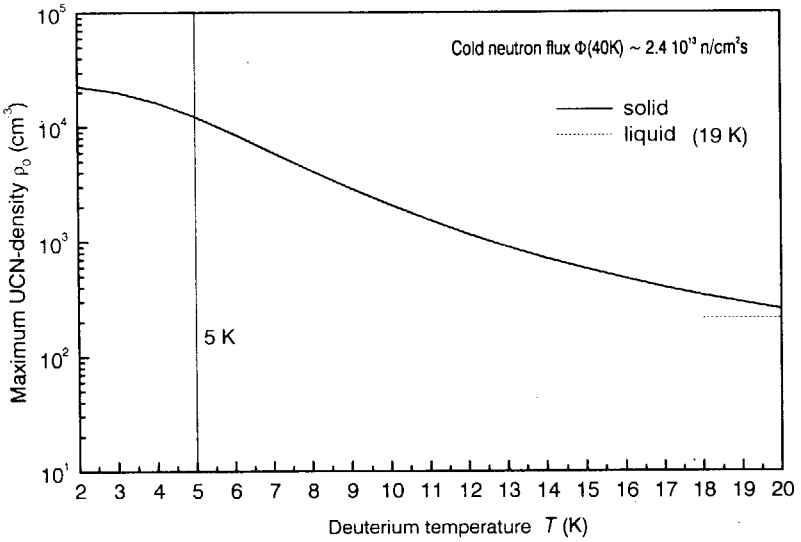

Fig. 2

Cross sections for absorption and up-scattering of neutrons with v=2200 m/s on ortho-D_2 as a function of the D_2 temperature

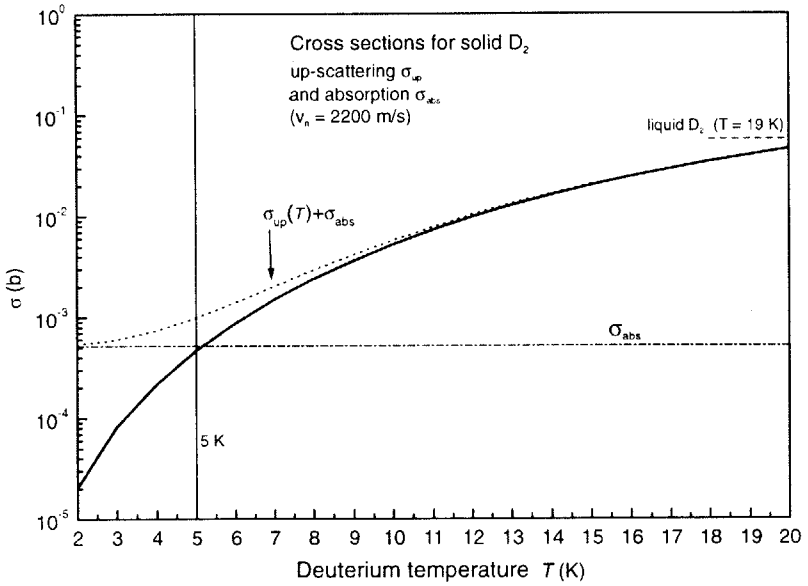

Fig. 3

Maximum UCN density in ortho-D_2 for a neutron flux $\Phi(T_n) \sim 2.4 \cdot 10^{13}$ n /cm^{2}s as function of the neutron temperature T_n, calculated from phonon spectra for three different D_2 temperatures

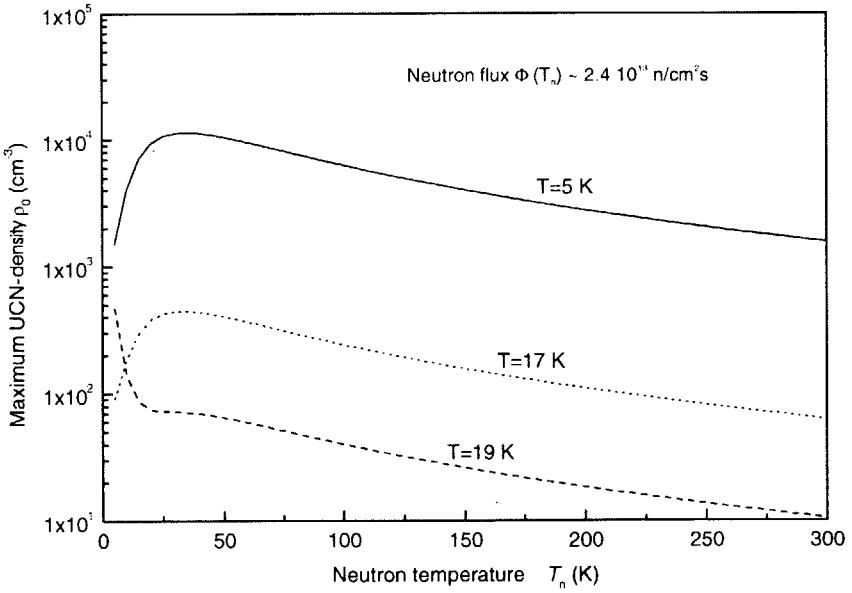

2.3 Experimental evidence for the production mechanism

Pioneering work from Gatchina

The rather high gain factors for UCN densities produced in solid D_2 at low temperature were investigated experimentally for the first time by Altarev et al. in 1980 in Gatchina [Alt80]. Figure 4, taken from [Alt80], shows in diagram (a), curve 2, the yield of UCN against the D_2 temperature. The gain factor for the yield at ~ 8 K compared to that at ~ 20 K is about 7, while the corresponding value calculated from Fig.1 gives about 20. The discrepancy may be explained by three facts: first the incoming neutron spectrum had a temperature of 300 K instead of 30 K, secondly no measures were taken to reduce the amount of para-D_2 in the converter, thirdly the H content, which strogly influences the gain, is not known.

Volume 80A, number 5,6 PHYSICS LETTERS 22 December 1980

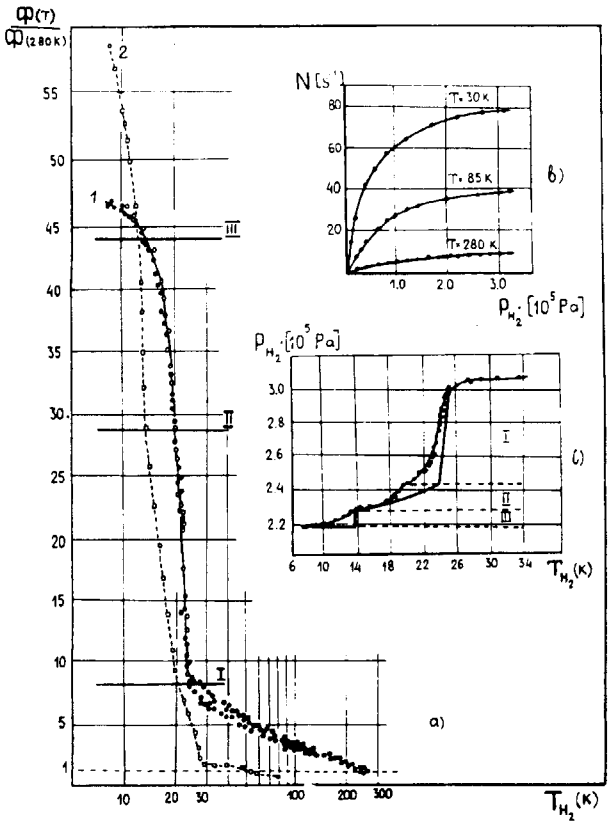

Fig. 1. (a) Curve 1: yield of UCN against temperature for hydrogen (○, experimental points obtained during cooling of the source; ●, experimental points obtained during heating of the source). Curve 2: yield of UCN against temperature for deuterium (□, experimental points obtained during cooling of the source). (b) Yield of UCN against hydrogen pressure at 280 K, 85 K, and 30 K. (c) Pressure of the ballast tank against temperature of the source. I Condensation phase; II phase attended by increase in liquid hydrogen pressure; III crystallization phase.

Fig. 4

UCN yield as a function of the D_2 temperature, from [Alt80]

Results from Los Alamos

Very recently UCN production in solid D_2 as function of the D_2 temperature was measured at the LANSCE accelerator at Los Alamos, where a pulsed 800 MeV proton beam impinging on a tungsten target produced 18 fast neutrons per proton [Car00]. These spallation neutrons were reflected back by Be blocks at 80 K and moderated to ~40 K by polyethylene. The inserted solid D_2 converter had a volume of up to 1 liter. Figure 5 from [Car00] shows the detected UCN against the D_2 temperature compared with calculations based on the same assumptions as above. The calculated values take into account a number of known and experimentally verified effects causing losses due to H impurities and contaminations with para-D_2. As Fig.5 shows, there is agreement between experiment and theory within a factor of 0.75, remaining unexplained so far.

Fig. 5

Measured and calculated UCN yield as a function of the D_2 temperature, from [Car00].

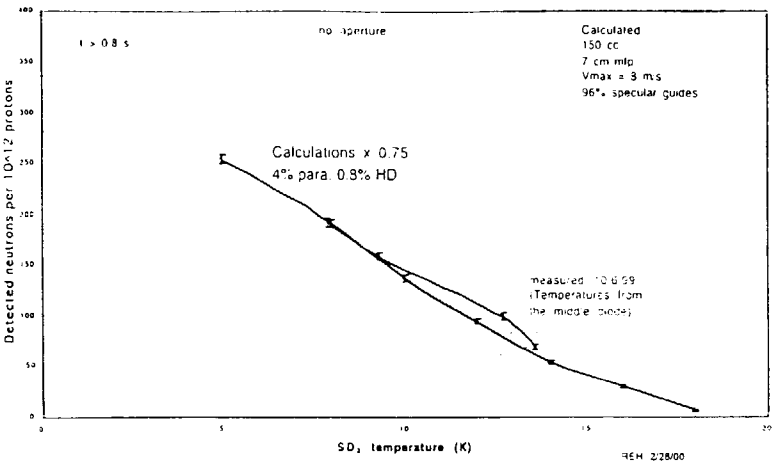

Figure A5.6. Measured and calculated temperature dependence of UCN yield from a 150 cc SD2 source. The temperature measurements plotted are taken from the diode thermometers on the UCN source. The calculations are plotted using a normalization factor of 0.75.

It has to be noted, that these results were obtained at a rather low primary neutron flux and thus at a low irradiation level. For the Mini-D_2 UCN source the continuous impinging neutron flux and γ radiation is expected to be at least an order of magnitude larger than the mean values at LANSCE.

2.4 The concept of Mini-D_2

The principle of Mini-D_2 based on solid D_2

Volume: 200 cm^3
Temperature: 5 K

The Mini-D_2 UCN source proposed for the FRM-II will be installed in the SR-4 beam tube, which is looking horizontally on the cold source. The flux of cold neutrons (effective temperature T_n ~ 40 K) is about $\Phi_n(40K)$ ~ 2.4 · 10^{13} n/cm^2s at the very end of SR-4 (see Appendix A.1).

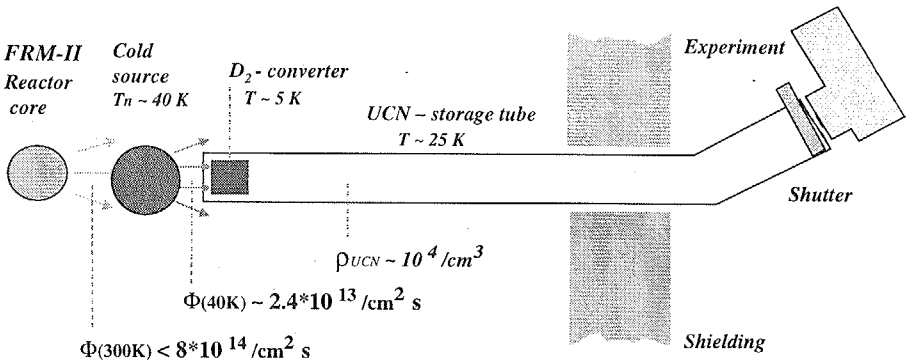

Fig. 6 Scheme of the Mini-D_2 UCN source

A schematic view of Mini-D_2 is shown in Fig.6. Mini-D_2 will have a rather small converter (~200 cm^3) of solid D_2 at a temperature of < 5 K. The converter is placed in a long evacuated tube, the UCN storage tube (diameter ~ 6 cm, length ~ 8 m, volume ~ 20 liter). One end of this tube (containing the converter block) is directed towards the cold source of the reactor, the other towards the experiments outside the reactor shielding. UCN produced in the converter can escape into the storage tube. Here an UCN density builds up, which is given by the equilibrium of the production rate in the converter with the total loss rate, consisting of (a) absorption and up-scattering in the converter, (b) losses during wall collisions (absorption or up-scattering), (c) decay, and possibly (d) escape through holes.

The converter is built up in the core-near end of the UCN storage tube by condensing D_2 gas at low pressure on the nose, which is kept at a temperature of < 5 K.

The inner walls of the UCN storage tube are covered at the inside with a thin layer of Be (repulsive potential U_{Be}= 252 neV). They have to be cooled to a temperature < 30 K to obtain wall losses as low as $5 \cdot 10^{-5}$ per collision [Age85, Alf92]. Furthermore, in order to keep diffuse reflection low the roughness of the surface should be smaller than the wavelength of the UCN (~100 nm).

At the outside end of the UCN storage tube, however still inside of the tube, a Be - covered shutter allows to extract the UCN through thin Al windows into the experiment, if required.

The UCN storage tube is inside of an evacuated cryostat tube. Both tubes together are moved as far as possible into the SR-4 beam tube.

2.5 UCN density calculations

The storage volume: buffer and guide

The UCN density in the storage tube will reach about the same magnitude as in the converter if the total losses in the storage-tube are small compared to those in the converter. The storage tube first works as a buffer, where the UCN can survive much longer than they would inside the converter, and, secondly, it transfers the high UCN density from near the converter to the experimental area.

The UCN density distribution in the tube may be calculated with the help of diffusion theory [Sei99]. Because of the constant cross section and cylindrical symmetry of the tube the variation along the axis may be described by a one-dimensional differential equation of second order with the coefficients depending on the part of the tube considered (converter, evacuated part). The parameters are the diffusion coefficients D and the effective storage time constants τ. The general solution for the case of stationary equilibrium is given by

$$\rho(x) = \alpha \cosh x/L + \beta \sinh x/L + \rho_0$$

UCN density calculations according to diffusion theory

Here ρ is the UCN density, x the coordinate along the axis of the tube, $L = (D\,\tau)^{1/2}$ the diffusion length, α and β are constants to be determined by appropriate boundary conditions, and ρ_0 is the (maximum) UCN density in the converter, without UCN escaping into the evacuated part of the storage tube (converter completely enclosed by reflecting walls).

Figure 7 shows typical results: the solid curve was calculated for a wall loss factor $\mu = 5 \cdot 10^{-5}$ and $f = 12.5\%$ diffuse reflection, the dashed curve for the same wall loss factor, but with $f = 50\%$ diffuse reflection, and the dotted curve for increased wall losses $\mu = 5 \cdot 10^{-4}$ and $f = 12.5\%$ diffuse reflection, as in the first case. All curves show a step in the density at the boundary between the converter and the evacuated part of the tube. This is caused by the fact, that UCN are produced at the potential $U_{D2} \sim 103$ neV and hence are accelerated when leaving the converter. As a consequence the momentum part of the phase space is enlarged by the factor η:

$$\eta = (1 - \kappa^3) \,/\, (1 - \kappa^2)^{3/2} = 1.61 \quad \text{with} \quad \kappa = (U_{D2}/U_{Be})^{1/2}$$

According to Liouville's theorem the six-dimensional phase-space density is equal on both sides of the boundary. Therefore the spatial density in the evacuated part has to increase by just the same factor $\eta = 1.61$ [1].

The solid curve in Fig. 7 for both, low losses and low diffuse reflection, shows only a slight decrease of the UCN density along the storage tube. The dashed curve shows the effect of enhanced backwards reflection. By this the probability increases to stay inside the strongly absorbing converter, thus reducing the total number of UCN, especially far away from the converter. The dotted curve reflects the drastically enhanced wall losses, which now determine the density drop along the axis of the evacuated tube and cause a general decrease, although only to roughly about 50% of the original values, because losses in the converter still predominate.

[1] The same result is obtained by calculating the portion of total reflected neutrons impinging in the evacuated volume onto the converter boundary [Tri98].

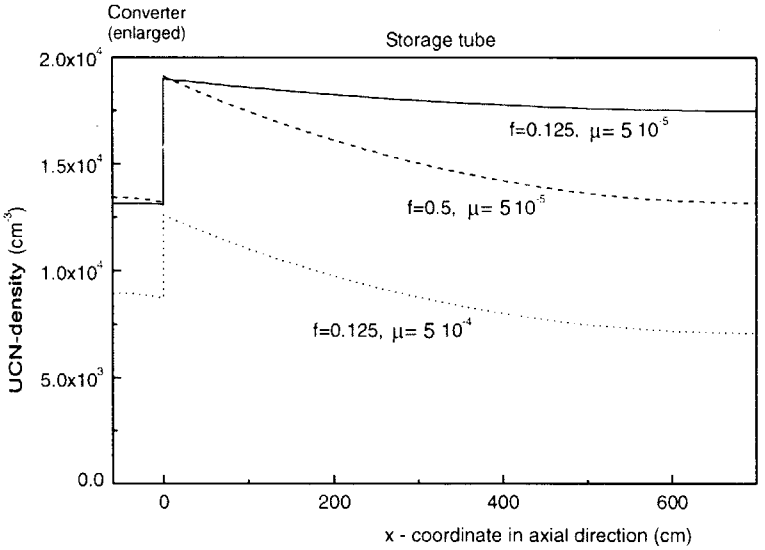

Fig. 7

UCN density distribution along the axis of converter and storage tube for different wall loss factors μ and diffuse reflection probabilities *f*

It is convenient to compare the losses in the various parts of the source by means of the respective storage time τ. In the D_2 converter at 5 K the up-scattering cross section corresponds to about 80% of the absorption cross section and the resulting effective storage time $\tau_{conv} \sim 0.08$ s. In the evacuated storage tube wall losses and β- decay cause $\tau_{evac} \sim 170$ s and $\tau_{evac} \sim 20$ s for $\mu = 5 \cdot 10^{-5}$ and $\mu = 5 \cdot 10^{-4}$, respectively. Taking into account that the neutrons stay in the evacuated tube ~1000 times longer than in the converter, we can explain the observed effects in Fig.7 quite well. The time constant for filling the storage tube with UCN from the converter is approximately given by $\tau_{conv} \sim 0.08$ s multiplied by the ratio of their effective volumes (~ 100), and the reciprocal ratio of average velocities (~ 4 / 6).

Design values:

$\rho \sim 10^4$ n / cm^3

$\Phi \sim 5 \cdot 10^5$ n/cm^{2}s

Generally the results from Fig.7 confirm the UCN densities expected of approximately 10^4 n/cm^3, even if 30% losses in the Al windows are taken into account [Sto78]. Results of Monte Carlo simulations are in excellent agreement with these analytical calculations [Lei99], [Sei99].

The upper limit of the UCN flux density Φ emerging from the converter into the evacuated tube in the continuous operation mode (open shutter at the far end) can be estimated from the balance of UCN production in the converter and UCN losses by a) absorption, b) up-scattering, and c) flow into the evacuated tube, assuming low wall losses and high specular reflectivity [Tri98]:

$$\Phi = \rho_0 \left(4 / v_{conv} + \tau_{conv} / l_{conv} \right)^{-1}$$

with $\rho_0 \sim 10^4$ n/cm^3 the UCN density in the converter without leakage, v_{conv} ~ 4 m/s the average UCN velocity in the converter, $\tau_{conv} \sim 0.08$ s and l_{conv} ~ 7 cm, the axial length of the converter. With these numbers one obtains $\Phi \sim 5 \cdot 10^5$ n/cm^{2}s.

2.6 An open question and preventive counter-measures

For achieving the design value of UCN density and flux, respectively, a crucial quantity is the effective storage time in the converter material, which was assumed to be τ_{conv} ~ 0.08 s. This value corresponds to absorption in solid D_2 and to up-scattering (~80 % of absorption at 5 K, see Fig.2). In order to prevent additional absorption, the D_2 has to be sufficiently clean. Based on the absorption cross sections shows we must ensure, that the atomic concentration of H is < 10^{-4} and that of N_2 < 10^{-5} e.g. to be of negligible influence. These requirements can be fulfilled if adequate precautions are taken.

An enhanced up-scattering can have various causes. It depends on the portion of para-D_2, and on the temperature. From Liu et al. [Liu99] one obtains for the lifetime due to up-scattering on a fraction x_{para} of the solid D_2 content of the solid D_2 [Liu99]:

$$\tau_{para} \sim 0.00147 / x_{para} \text{ [s]}$$

In order to get $\tau_{para} >> \tau_{conv}$ ~ 0.08 s, the fraction of para- D_2 should be $x_{para} < 5 \cdot 10^{-3}$. This can be obtained from natural D_2 (for which, at room temperature, x_{para} = 1/3) by storing the D_2 at a temperature < 20 K for a period of several months [Sil80]. In addition, intense radiation seems to drive the D_2 into the ortho state, as is indicated from experiments by the group at PNPI in Gatchina [Car00].

Of crucial importance: the thermal conductivity of the D_2 converter

The temperature of solid D_2 is given by the heat load due to irradiation and by the thermal conductivity. The heat load is on the average P_{in} ~ 0.14 W/cm^3 inside the nose of SR-4, where the converter will be placed [Gau99]. The thermal conductivity depends firstly on the phonon density and thus temperature and secondly on the fraction of para - D_2 and other scattering centers for phonons. Figure 8 shows the thermal conductivity $\lambda(T)$ of D_2 for different values of x_{para} as a function of the temperature [Gor81]. The maximum at T ~ 4 K is a consequence of the density of phonons and phonon – phonon scattering, both increasing with temperature.

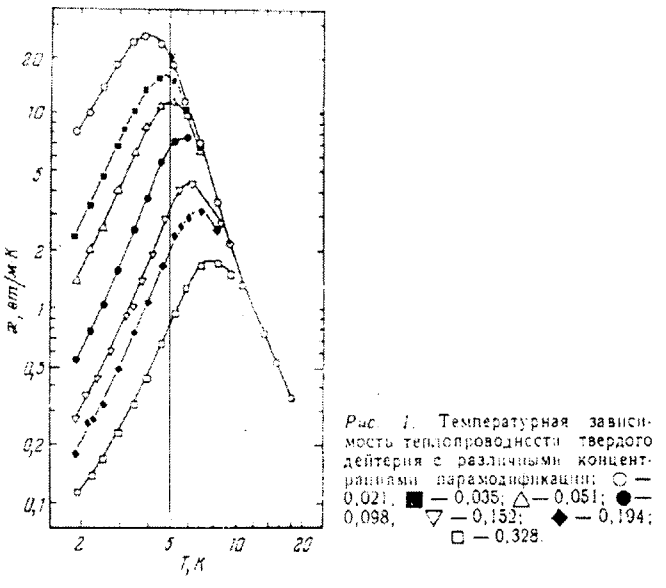

Рис. 1. Температурная зависимость теплопроводности твердого дейтерия с различными концентрациями парамодификации: ○ — 0,021; ■ — 0,035; △ — 0,051; ● — 0,098; ▽ — 0,152; ◆ — 0,194; □ — 0,328.

Fig. 8

Thermal conductivity of solid D2 as a function of temperature for para fractions x from 2.2% to 33%, from [Gor81].

The maximum value may be reduced drastically by additional scattering centers, for instance by radiolysis effects, by para - D_2 production, or simply by mechanical cracks. While the last two causes can be considered to be controllable, the effects of radiolysis are not sufficiently well known at present. Measurements at LANSCE of the UCN production rate as a function of the primary proton pulse intensity showed no deviation from the expected linear dependence so far [Car00]. Care has to be taken, however, when trying to transfer and extrapolate to the present situation. At best the maximum pulses in that experiment correspond to an irradiation intensity an order of magnitude smaller at Mini-D_2.

Maximum temperature controllable by cold finger

In order to prevent the reduction of thermal conductivity by additional phonon scattering centers, the cooling of the D_2 converter has to be optimized. Therefore the D_2 is contained in a cylinder jacket with inner and outer radii r_i and r_o, respectively, formed by two coaxial, double-walled tubes with He gas as coolant between the walls, keeping them at a temperature of $T_w < 5$ K. Assuming infinite length of the tubes and constant thermal conductivity, one obtains with $\Delta r = r_o - r_i$ the maximum temperature:

$$T(r_m) = T_w + \Delta r^2 P_{in} / (8 \lambda) \quad \text{at} \quad r_m = (r_i + r_o) / 2$$

This shows that a reduction in λ could be compensated very effectively by a corresponding reduction in Δr^2. Of course, a decreased converter volume also causes less UCN to be produced. However, the gain factor for λ is $(1 - r_i / r_o)^{-2} = 4$ for $r_i / r_o = ½$ e.g., while the reduction of the converter volume then is $(1 - r_i^2 / r_o^2) = ¾$ only. The optimum value for r_i at given r_o can be determined by experiment under the real conditions.

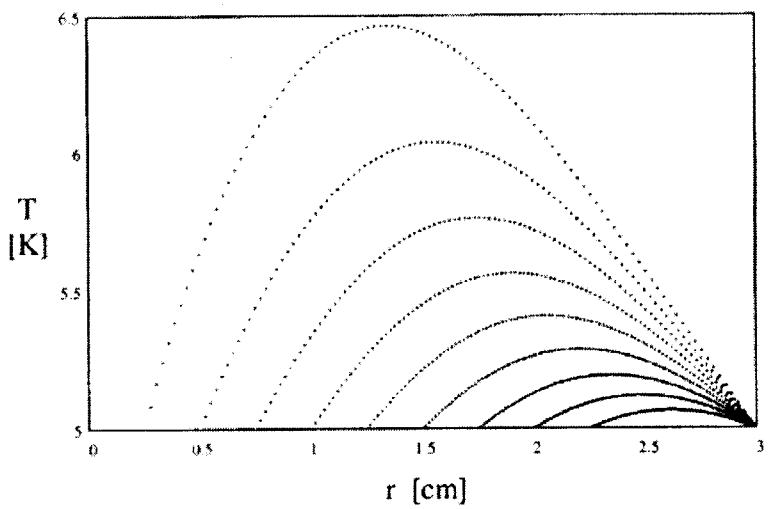

Fig. 9
Radial temperature profiles.
Outer radius r_o fixed.
Parameter: radius r_i of cold finger.

Figure 9 shows the radial temperature profiles calculated for fixed r_o = 3 cm and different values for r_i, with T_w = 5 K and λ assumed to be temperature dependent: $\lambda(T) \sim 18.75 / T^3$ [W / cm K], corresponding to the common right branches of the curves in Fig. 8. These temperature profiles can be understood rather well with the approximate relationship given above.

3. The technical design

Positive preliminary approval by the technical experts (TÜV)

The technical design of the Mini-D_2 UCN source, as described in this report, takes into account all safety aspects to be expected at FRM II as a nuclear installation. The design was examined by the experts of the technical safety authorities (TÜV) with the result that it could be approved in case of an official request, which will be submitted, however, only after the third partial construction license for the reactor itself has been obtained.

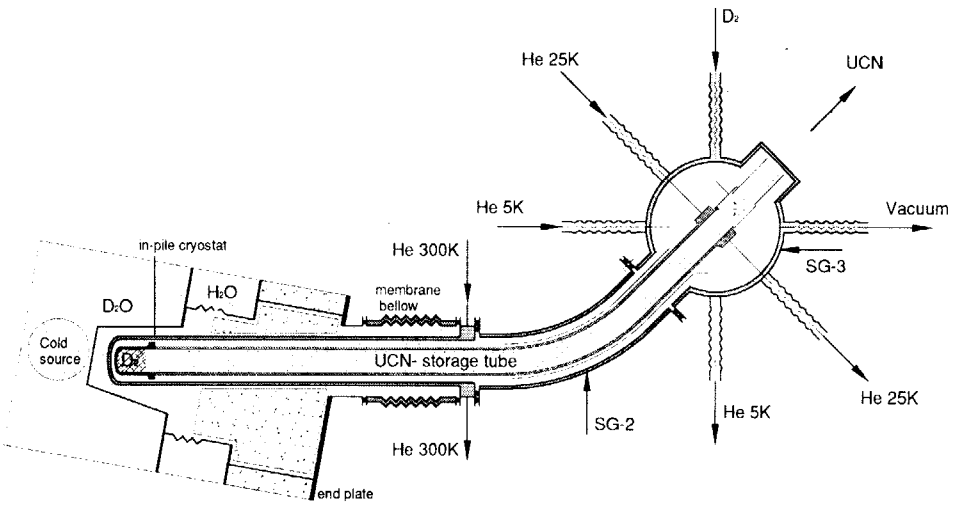

Fig. 10
Scheme of the mechanical design

Figure 10 shows a schematic view of the Mini-D_2 UCN source inside the beam tube SR-4. From left to right we find:

- the cold source inside the D_2O moderator,
- the SR-4 beam tube crossing the biological shield and the H_2O pool, closed by
- the end plate of SR-4, which has a hole for
- the double-walled in-pile cryostat (colored in green), connected to the end plate via a double-walled membrane bellow (light green), and to the other side followed by
- the double-walled, curved cryostat tube (bending radius 1.5 m, angle 50°, He gas protected), which brings the system out of the direct irradiation flux, finally ending with
- the double-walled, He gas protected cylindrical end vessel (diameter ~ 60 cm, height ~ 1 m) with feeders for coolants, vacuum pumping and D_2 gas and thin Al windows for UCN;
- the cryostat houses the double-walled UCN storage tube (purple) with the cup (blue) containing in the maximum ~ 200 cm^3 of solid D_2 as converter (green, hatched) at the very end near the cold source, and with a shutter and a thin Al window at the other end. The total length of the storage tube is 8 m, the inner diameter ~57 mm, and the volume ~ 20 liter.

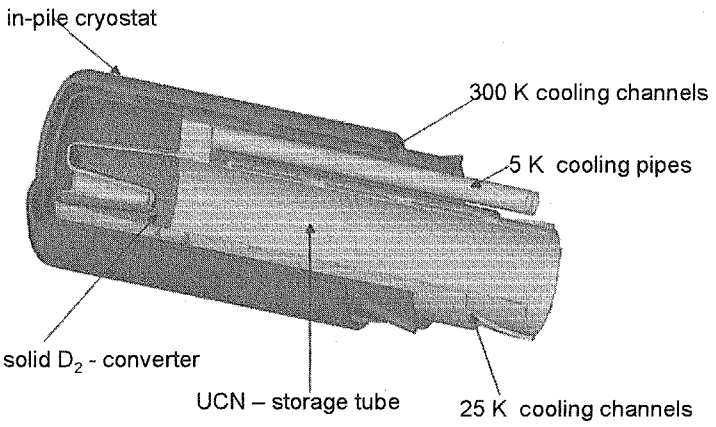

Fig. 11
Cut away- view of the source with the converter

Technical details

Figure11 shows a cut-away view of the end piece of the in-pile part of the Mini-D_2 UCN source close to the cold source. It is inserted in the SR-4 beam tube, which contains He protection gas (130 kPa). The (orange) double-walled cryostat of the source (outer diameter ~108 mm, inner diameter ~ 99 mm, wall thickness 3 mm respectively 2 mm) is made of Zirkaloy ZR4. This material has high yield strength even at the maximum temperature of 700 °C, which would only be achieved in case of a cooling failure. The cooling of the inpile crystat is provided by He gas (~300 K) being pumped through the gap between the walls.

Inside the evacuated cryostat the (yellow) double-walled UCN storage tube is installed. This tube is made of Al6061, an aluminum alloy especially suited to withstand high irradiation levels in a nuclear reactor environment (outer diameter ~65 mm, inner diameter ~57 mm, wall thickness 0.8 mm each). The very end of the storage tube has a coaxial finger (length ~ 50 mm) to improve the cooling of the solid D_2 converter, which will be condensed into this part of the tube (green). The cup containing the converter will be cooled by supercritical He (single phase only, maximum pressure ~300 kPa, temperature < 5 K), provided by separate tubes (diameter ~ 12 mm). The rest of the storage tube is cooled by He gas at ~ 25 K flowing at a pressure of ~ 300 kPa in the gap between the walls.

The D_2 condensed into the cup at low temperature (< 5 K) will expand, when warmed up. Between 5 K and the melting temperature (18.7 K) the density decreases by about 3 %. To prevent the converter cup and the central cooling finger from rupturing they are formed slightly conical, so that the solid expanding D_2 can slide out in axial direction.

The inner surface of the storage tube will be polished to achieve good specular reflectivity, then plated with Ni, and finally sputtered with Be. The Ni layer is needed, because Be sputtered directly on Al would not form absolute complete coating.

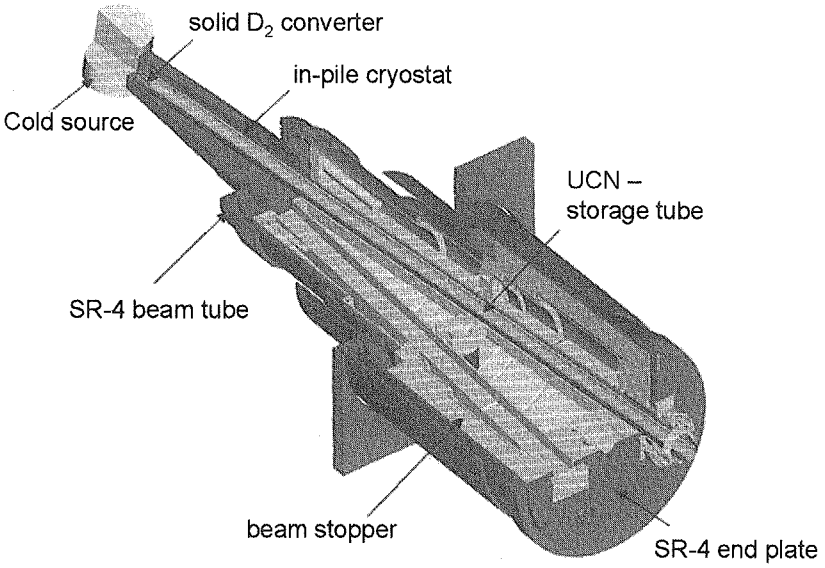

Fig. 12
Cut away- view of the SR-4 beam tube with the in-pile part of the source

Figure12 shows a cut-away view of the SR-4 beam tube with the cold source at one end and the SR-4 end plate in the experimental hall. The Mini-D_2 in-pile cryostat with the UCN storage tube penetrates the end plate.

UCN source movable in axial direction by 1.8 m

Outside the end plate another about 2 m long straight part of the in-pile cryostat is running inside a long double-walled membrane bellow, which closes the He protection gas volume in the SR-4 beam tube and thus represents a barrier against water loss of the reactor pool in case of a break of the SR-4 beam tube. The space between the walls of the bellow is filled with He protection gas. Pressure loss would indicate a leakage of one of the walls of the bellow. The length of the bellow can be varied by 180 cm. By this the in-pile part of the UCN source may be withdrawn from the high radiation level region back into the internal shielding block of the SR-4 in order to save cooling, if the UCN source is not operating. The He protection volume of the SR-4 needs not to be opened during this procedure. The outer part of the cryostat, the end vessel as well as parts of the surrounding shielding, the D_2 gas handling system and the cryostat with the secondary cooling circuits (see below) will be moved at the same time. Plan views of the experimental hall for both positions are shown in Figures 13 a) and b).

The flow-diagram of the whole system including the deuterium gas handling system and the cooling circuits is described in Appendix A.5. Here also some safety aspects are listet.

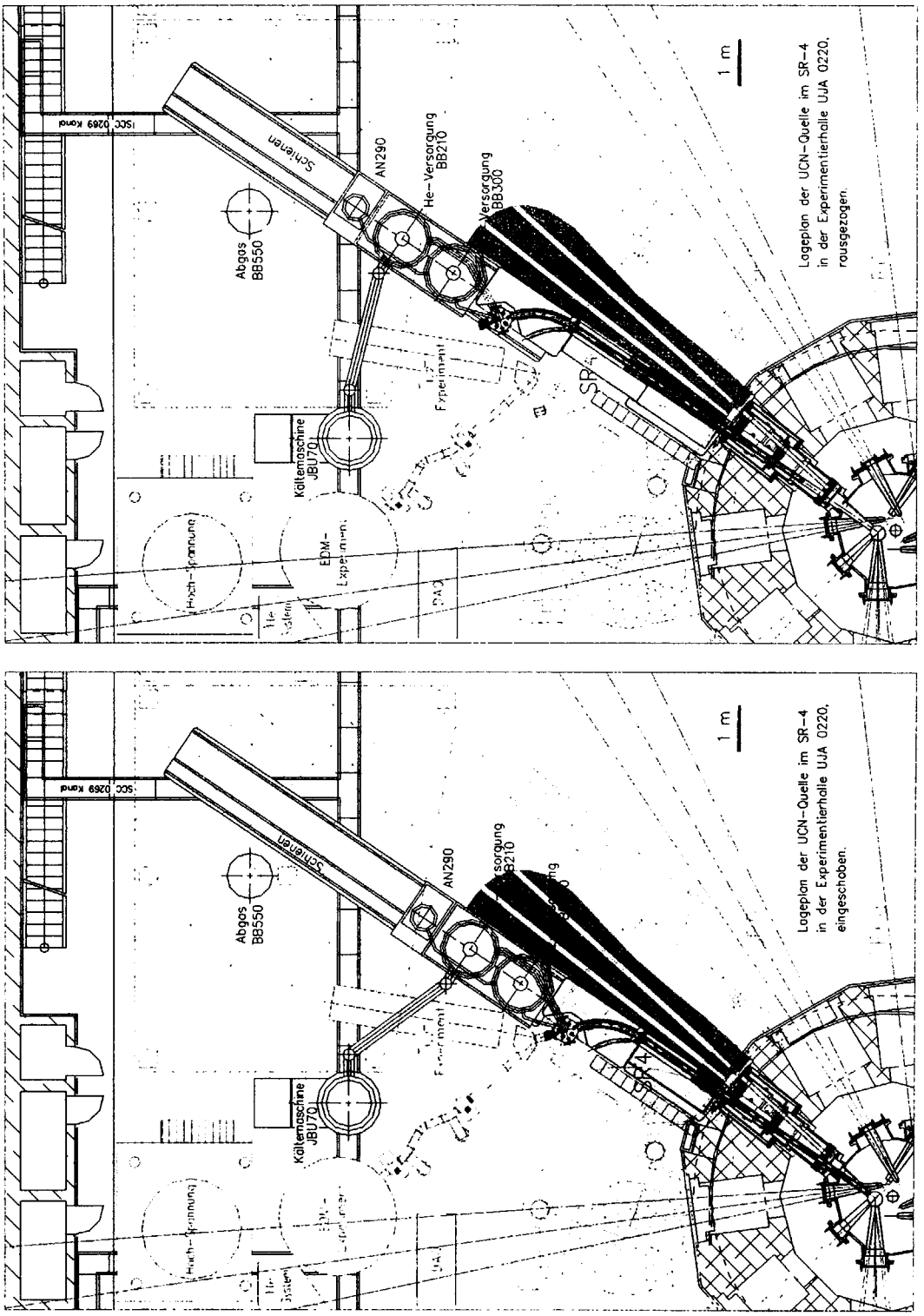

Fig. 13 Plan views of the experimental hall, a) with the source completely moved into the SR-4 beam tube, b) withdrawn by 1.8 m.

4. Status of the project

4.1 Project progress

According to the project time schedule shown in table 1 and 2 five different stages are defined for each of the seven sub-projects. These stages are:

1. Conception
2. Design
3. Construction documents
4. Construction
5. Tests / Commissioning

In the following list short comments on each sub-project are given.

- Mini-D_2: It includes the complete UCN storage tube and the cryostat (in-pile part, bended part, and cylindrical end vessel).
- SR-4 (internal) beam stopper: The standard beam stopper had to be replaced by a stopper with enlarged cross sections for the UCN source. The modified stopper and end plate is ready for being installed.
- D_2-gas handling: It includes the D_2-gas storage, the small cryo-plant for converting the para- into the ortho-D_2, and the vacuum-system of the source.
- D_2-Test-cryostat: This is a He-gas protected cryostat for preparatory investigations of the D_2-converter and alternative materials. It serves the testing of the prototype UCN storage tube and its cooling circuits, to study the influence of high γ irradiation on the thermal conductivity using the bremsstrahlung from the 2.3 GeV-electron synchrotron in Bonn, to study the UCN-production at a pulsed TRIGA-reactor in a collaboration with the University of Mainz (see below). The construction of the test-cryostat is almost completed.
- Be-sputtering laboratory: A new sputtering device is being installed allowing surface coatings by different materials e.g. beryllium, to meet the various requirements on well-defined surfaces needed for handling UCN. The sputtering device is under commissioning.
- Cryo plant: It includes the primary refrigerator, the 5 K and 25 K secondary cooling circuits, the 300 K circuit, and all He gas storage capacities.
- Infrastructure: It includes the external shielding and the carriage system to remove the source from the high level radiation region.

At present the overall progress of the project is already beyond the 50 % mark. This includes the following topics:

- The design of the source is completed
- All relevant parameters are fixed
- Calculations were made on following topics:
  - UCN-densities
  - Neutron fluxes
  - γ fluxes
  - Heat load
  - Heat removal
  - Maximum temperatures
  - Mechanical stability
  - Tritium activation
  - Shielding (in progress)
- Technical design is in progress
- System description is in progress
- Flow-diagram is in progress
- Internal SR-4 beam stopper and end plate is ready for installation
- Technical developments for construction of the UCN storage tube, the converter cell, and the in-pile cryostat are under way
- Be sputter device is under commissioning
- Test cryostat for preparatory investigations of D_2 as converter is almost complete
- A program for experiments at the Mini-D_2 UCN source is under way

4.2 Time schedules

Table 1 shows a correlation schedule of all parts of the project with the different stages. Table 1 gives the time schedule. It shows that the commissioning of the source is expected to occur during the first half of year 2003. For this the commissioning of the FRM II is assumed to take place in time.

Informations on manpower, collaborations and cost estimate are summarized in Appendix A.6.

Tab. 1 Project progress

	Task	Target start date	Target end date	Portion of progress	Actual start date	Actual end date	Actual progress	Total
1	**Conception**							
1.1	Mini-D2	01.01.99	01.04.00	4,00%	01.01.99	01.04.00	4,00%	
1.2	SR-4 bear	01.01.99	01.01.00	3,00%	01.01.99	20.12.99	3,00%	
1.3	D2-Gasha	01.01.99	01.01.00	3,00%	01.01.99	20.12.99	3,00%	
1.4	D2-Testcry	01.01.99	01.01.00	2,00%	01.01.99	20.12.99	2,00%	
1.5	Be-sputter	01.01.99	01.01.00	2,00%	01.01.99	20.12.99	2,00%	
1.6	Cryo plant	01.01.99	01.04.00	3,00%	01.01.99	01.04.00	3,00%	
1.7	Infrastructu	01.01.99	01.04.00	3,00%	01.01.99	02.01.99	3,00%	
	Conceptior	*01.01.99*	*01.04.00*	*20,00%*	*01.01.99*	01.04.00	*20,00%*	20,00%
2	**Design**							
2.1	Mini-D2	01.04.99	01.07.00	4,00%	01.07.99		3,50%	
2.2	SR-4 bear	01.04.99	01.01.00	3,00%	01.07.99	20.12.99	3,00%	
2.3	D2-Gasha	01.04.99	01.04.00	3,00%	01.04.99	01.04.00	3,00%	
2.4	D2-Testcry	01.04.99	01.01.00	2,00%	01.03.99	20.12.99	2,00%	
2.5	Be-sputter	01.04.99	01.01.00	2,00%	01.04.99	20.12.99	2,00%	
2.6	Cryo plant	01.04.99	01.07.00	3,00%	01.04.99		2,00%	
2.7	Infrastructu	01.04.99	01.07.00	3,00%	01.04.99		2,50%	
	Design tota	*01.04.99*	*01.07.00*	*20,00%*	*01.03.99*		*18,00%*	38,00%
3	**Construction documents**							
3.1	Mini-D2	01.03.00	01.01.01	4,00%	01.03.00		1,00%	
3.2	SR-4 bear	01.01.00	01.04.00	3,00%	01.01.00	01.04.00	3,00%	
3.3	D2-Gasha	01.03.00	01.11.00	3,00%	01.03.00		1,00%	
3.4	D2-Testcry	01.09.99	01.01.00	2,00%	01.09.99	01.11.99	2,00%	
3.5	Be-sputter	01.09.99	01.01.00	2,00%	01.11.99	31.12.99	2,00%	
3.6	Cryo plant	01.07.00	01.01.01	3,00%	01.04.00		0,50%	
3.7	Infrastructu	01.07.00	01.01.01	3,00%	01.04.00		0,50%	
	Documents	*01.09.99*	*01.01.01*	*20,00%*	*01.03.99*		*10,00%*	48,00%
4	**Construction**							
4.1	Mini-D2	01.02.01	01.07.02	4,00%			0,00%	
4.2	SR-4 bear	01.04.00	01.09.00	3,00%	01.04.00		2,50%	
4.3	D2-Gasha	01.02.01	01.04.02	3,00%			0,00%	
4.4	D2-Testcry	01.01.00	01.10.00	2,00%	01.02.00		1,50%	
4.5	Be-sputter	01.01.00	01.07.00	2,00%	01.01.00	01.04.00	2,00%	
4.6	Cryo plant	01.02.01	01.07.02	3,00%			0,00%	
4.7	Infrastructu	01.02.01	01.07.02	3,00%			0,00%	
	Constructio	*01.01.00*	*01.07.02*	*20,00%*			*6,00%*	54,00%
5	**Tests/Commissioning**							
5.1	Mini-D2	01.09.02	31.12.02	4,00%			0,00%	
5.2	SR-4 bear	01.09.00	01.10.00	3,00%			0,00%	
5.3	D2-Gasha	01.05.02	01.10.02	3,00%			0,00%	
5.4	D2-Testcry	01.11.00	01.01.01	2,00%			0,00%	
5.5	Be-sputter	01.09.00	01.10.00	2,00%			0,00%	
5.6	Cryo plant	01.09.02	31.12.02	3,00%			0,00%	
5.7	Infrastructu	01.09.02	31.12.02	3,00%			0,00%	
	Tests/Com	*01.09.00*	*31.12.02*	*20,00%*			*0,00%*	**54,00%**
	Total			100,00%				

	98	1999				2000				2001				2002				2003				
Task	O,N,D	J,F,M	A,M,J	J,A,S	O,N,D	J,F,M	A,M,J	J,A,S	O,N,D	J,F,M	A,M,J	J,A,S	O,N,D	J,F,M	A,M,J	J,A,S	O,N,D	J,F,M	A,M,J	J,A,S	O,N,D	
Conception	####	4,00%	4,00%	4,00%	4,00%	4,00%	####															
Subtotal						20%																
Design		####	4,00%	4,00%	4,00%	4,00%	4,00%	####														
Subtotal							20%															
Construction documents			####	4,00%	4,00%	4,00%	4,00%	4,00%	4,00%	####												
Subtotal									20%													
Construction				####	2,00%	2,00%	2,00%	2,00%	2,00%	2,00%	2,00%	2,00%	2,00%	2,00%	2,00%	####						
Subtotal														20%								
Tests, commissioning							####	2,22%	2,22%	2,22%	2,22%	2,22%	2,22%	2,22%	2,22%	2,22%	2,22%	####				
Subtotal																	20%					
Total																	100%					
Project progress (F)																						
Date	####	31.3.99	####	####	####	31.3.00	####	####	####	31.3.01	30.6.01	30.9.01	31.12.01	31.3.02	####	####	####	31.3.03	####			
Target	0%	4,00%	12,00%	20,00%	32,00%	46,00%	56,00%	62,00%	70,22%	74,44%	78,66%	82,88%	87,10%	91,32%	95,54%	97,76%	99,98%	100%				
Actual progress					32,00%	45,00%	54,00%															

Tab. 2

Time schedule

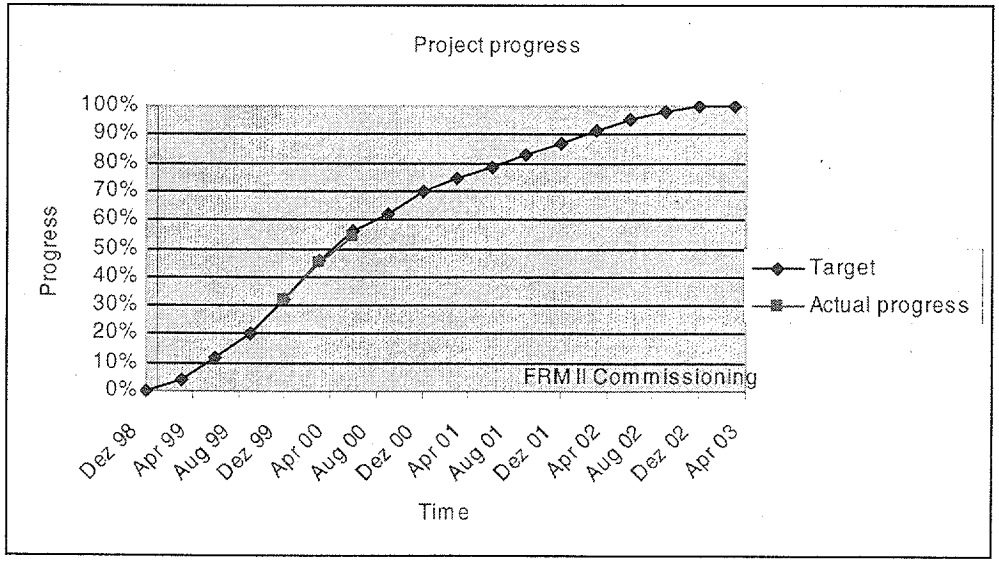

References

[Age85] P. Ageron *et al.*, Z. Phys. B – Cond. Matter **559**, 261 (1985).
[Alf92] V.P. Alfimenkov *et al.*, JETP Lett. **55**, 84 (1992).
[Alt80] I.S. Altarev, *et al*, Phys. Lett. A **80**, 413 (1980).
[Alt92] I.S. Altarev, *et al.*, Phys. Lett. B **276,** 242 (1992).
[Alt96] I.S. Altarev, *et al.*, Physics of Atomic Nuclei **59**, 1152 (1996).
[Arz86] S.S. Arzumanov *et al.*, JETP Lett. **44**, 271 (1986).
[Car00] R. Carr *et al.*, Technical Review Report, Los Alamos Neutron Science Center, 11 April 2000.
[Gau99] W. Gaubatz, PhD Thesis, Phys. Dep. E21, Techn. Univ. München, 1999.
[Gol83] B. Golub and K. Böning, Z. Phys. B**51**, 95 (1983).
[Gor81] B.Ya. Gorodilov *et al.*, Fiz. Niz. Temp. **7**, 424 (1981).
[Küg78] K.-J. Kügler, W. Paul, and U. Trinks, Phys. Lett. **72B**, 422 (1978).
[Küg79] K.-J. Kügler, W. Paul, and U. Trinks, IEEE Trans. Nucl. Sci. **26**, 3152 (1979).
[Küg85] K.-J. Kügler, K. Moritz, W. Paul, and U. Trinks, Nucl. Instr. Methods **228**, 240 (1985).
[Lei99] R. Leisibach, Monte Carlo code ucndensity, see [Sei99]
[Liu99] C.-Y. Liu *et al.*, Appendix 12 in [Car00]
[Mam89] W. Mampe *et al.*, Phys. Rev. Lett. **63**, 593 (1989).
[Mam93] W. Mampe *et al.*, JETP Letters **57**, 82 (1993).
[Mic97] A. Michaudon, Report LA-13197-MS, Los Alamos National Laboratory, 1997.
[Nes92] V.V. Nesvizhevskii *et al.*, Sov. Phys. JETP **75**, 405 (1992).
[Pau51] W. Paul, in *Proc. Int. Conf. on Nucl. Phys. and Phys. of Fundam. Part.*, Chicago, 1951.
[Pau78] W. Paul and U. Trinks, in *Fundamental Physics with reactor neutrons and neutrinos*, ed. by T. von Egidy, IOP Conference Series 42, Bristol&London, 1978.
[Pau89] W. Paul, F. Anton, L. Paul, S. Paul, and W. Mampe, Z. Phys. C **45**, 25 (1989).
[Sei99] Ch. Seidel, Diploma thesis, Phys.-Dep. E18, Techn. Univ. München, Nov.1999.
[Ser94] A. Serebrov, *et al.*, JETP Lett. **59**, 757 (1994).
[Ser95] A. Serebrov, *et al.*, JETP Lett. **62**, 785 (1995).
[Ser97] A. Serebrov, *et al.*, Russian Academy of Sciences, PNPI, Preprint NP-57-1997 2200 (1997).
[Sil80] I.F. Silvera, Rev. Mod. Phys. **52**, 393 (1980).
[Smi90] K.F. Smith *et al.*, Phys. Lett. B **234**, 91 (1990).
[Ste80] K.A. Steinhauser *et al.*, Phys. Rev. Lett. **44**, 1306 (1980).
[Ste83] A. Steyerl *et al.*, Z. Phys. B **50**, 281 (1983).
[Ste88] A. Steyerl *et al.*, Rev. Phys. Appl. **23**, 171 (1988).
[Ste92] A. Steyerl *et al.*, in Neutron Optical Devices and Applications, edited by C.F. Majkzak and J. Woods, (SPIE, Bellingham, Washington, 1992).
[Sto78] A.D. Stoica and A.V. Strelkov, Nucl. Instr. Meth. **157**, 477 (1978).
[Tri98] U. Trinks, Internal Report, Phys.-Dep. E18, Techn. Univ. München, tu-25.02.98 (1998).
[Tri00] U. Trinks, F.J. Hartmann, S. Paul, and W. Schott, Nucl. Instr. Meth. A 440, 666 (2000).
[Yu86] Z-Ch. Yu, S.S. Malik, and R. Golub, Z. Phys. B - Cond. Matter **62** 137 (1986) .

Appendix A.1

Neutron fluxes in FRM II beam tube SR-4

Results of Monte Carlo calculations of neutron fluxes along the axis of beam tube SR-4 in FRM II without any installations by W. Gaubatz (13.10.98).

For four different energy sections, as a function of the distance r [cm] from the centre of the cold source.

Neutron flux F in 10^{11} n / cm^2 sec

Energy sections:

k=0 : <4.5 meV
k=1 : 4.5 meV < E < 625 meV (thermal)
k=2 : 625 meV < E < 821 keV
k=3 : 821 keV < E < 14.9 MeV

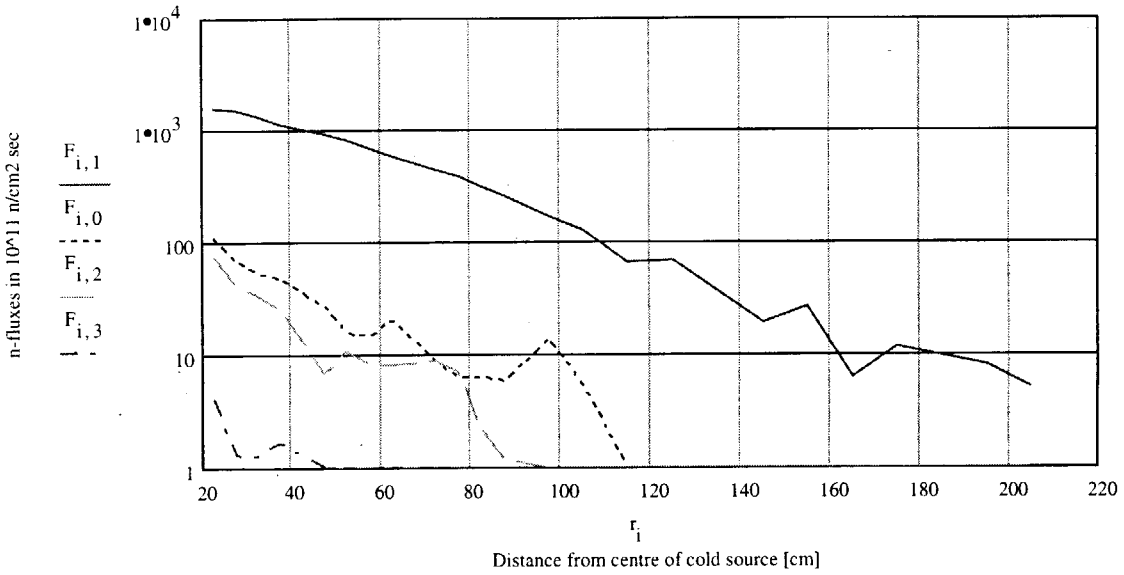

Appendix A.2

Tritium production in Mini-D2 converter

Deuterium quantity : 40 g = 10 mol = N_d = 12.04 10^{24} D-atoms
Mean distance from the centre of cold source: r = 22.5 cm

Thermal neutron flux at r = 22.5 cm : Φ_{therm} = 1.6 10^{14} n / cm^2 s

Absorption cross-section for v = 2200 m/s : σ_{abs} = 5.2 10^{-28} cm^2

Reactor cycle: t_{cycl} = 73 days
Irradiation time per year: 5 x 52 = 260 days
Irradiation time / total time: ε = 260 / 365

Tritium-decay-coefficient: $\lambda = \ln 2 / T_{1/2} = 1.78\ 10^{-9}$ / s

Number of Tritium-nuclei as a function of time: $Ntl_i := \frac{\sigma \cdot \Phi \cdot Nd \cdot \varepsilon}{\lambda} \cdot \left(1 - e^{-\lambda \cdot t_i}\right)$

Tritium-activity in Bequerel: $dNtl_i := \lambda \cdot Ntl_i \quad s^{-1}$

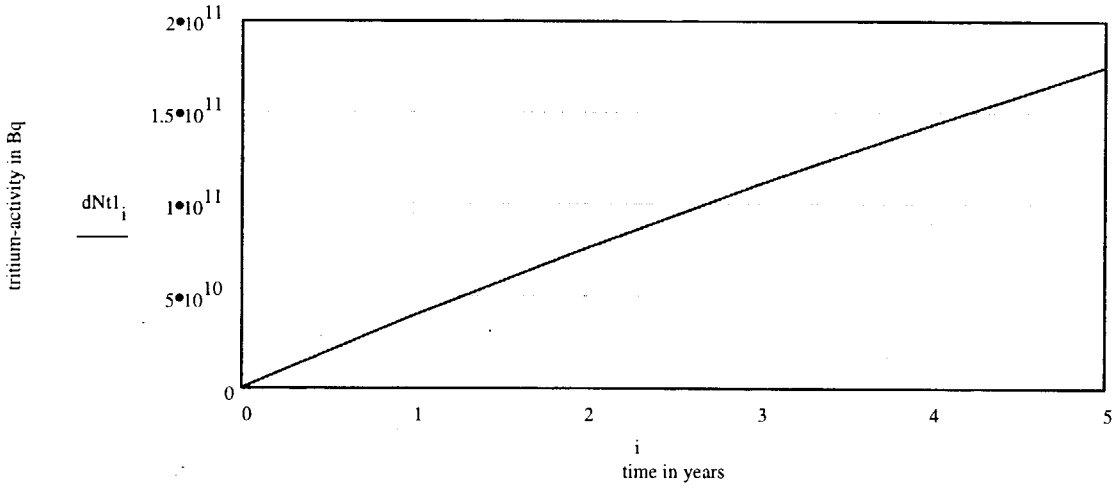

Result: Per reactor cycle a tritium-activity of 7.8 10^9 Bq would be produced in the D2-converter, if the D2 would be irradiated all the time. After four years the activity would be 1.4 10^{11} Bq. If then would occur an accident, so that all of the D2 would enter the gas collecting vessel JBU55 BB550 of the exhaust system and then 1/5 of that further into the exhaust chimney, then the tritium-activity released into the environment would still stay below the admissible activity limit of 3 10^{10} Bq (per one day).

Appendix A.3

Tritium production in liquid helium coolant of Mini-D2

^{4}He-quantity : 5kg = 1250 Mol = $N_{He4} = 75\ 10^{25}$

^{3}He-atoms (fraction in commercial He: 0.3 10^{-6}) : $N_{He3} = 22.5\ 10^{19}$

Irradiated fraction : $\kappa = 0.02$

Irradiated section (from centre of cold source) : $r = 20$ bis 210 cm

Mean thermal neutron flux in this section : $\Phi_{therm} = 3.36\ 10^{13}$ n/cm^{2}s

Absorption cross-section of ^{3}He (v = 2200 m/s, E_n=25meV) : $\sigma_{abs} = 5.33\ 10^{-21}$ cm^2

Tritium-decay-coefficient : $\lambda = \ln 2 / T_{1/2} = 1.78\ 10^{-9}$ / s

Reactor cycle : $t_{cycl} = 73$ days

Time of irradiation per year : 5 x 52 = 260 days

Time of irradiation / total time : $\varepsilon = 260 / 365$

Tritium is created by neutronen-capture in ^{3}He. Then tritium decays creating again ^{3}He.

Tritium-nuclei as a function of time: $Nt2_i := \frac{\sigma \cdot \Phi \cdot \kappa \cdot \varepsilon \cdot NHe3}{\sigma \cdot \Phi \cdot \kappa \cdot \varepsilon + \lambda} \cdot \left[1 - e^{-(\sigma \cdot \Phi \cdot \kappa \cdot \varepsilon + \lambda) \cdot t_i}\right]$

^{3}He-nuclei as a function of time: $Nhe3_i := \frac{NHe3}{\sigma \cdot \Phi \cdot \kappa \cdot \varepsilon + \lambda} \cdot \left[\lambda + \sigma \cdot \Phi \cdot \varepsilon \cdot e^{-(\sigma \cdot \Phi \cdot \kappa \cdot \varepsilon + \lambda) \cdot t_i}\right]$

Tritium-activity in Bequerel: $dNt2_i := \lambda \cdot Nt2_i$

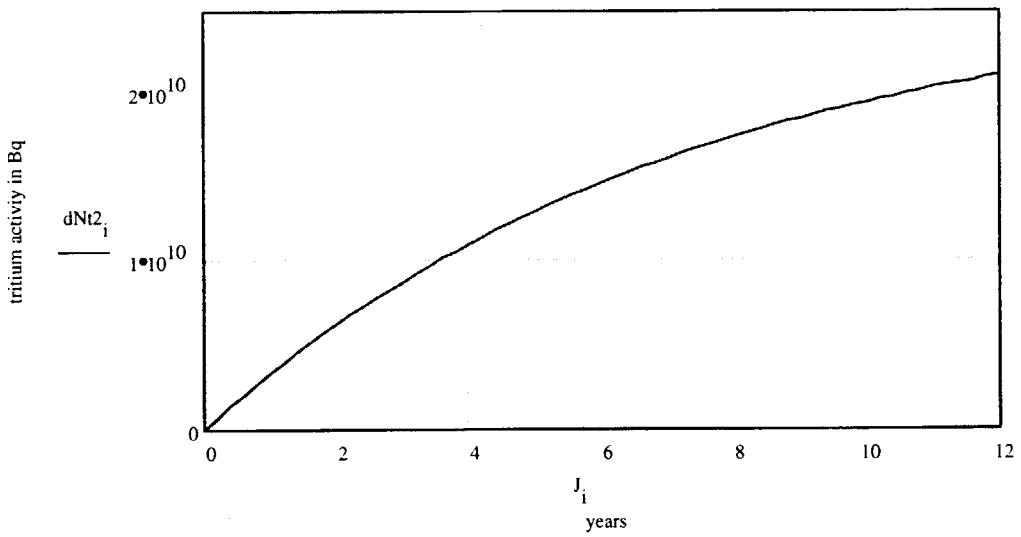

Result: After 12 years of permanent irradiation the tritium-activity in the liquid He coolant would be still considerably smaller than the admissible activity limit of 3 10^{10} Bq (per one day).

Appendix A.4

Heat input by irradiation in zircaloy ZR4

Specific heat input P [W/G] by β, γ and neutron radiation in zircaloy ZR4 along the axis of beam tube SR-4 in FRM II as a function of the distance r [cm] from the centre of the cold source, according to Monte Carlo calculations by W. Gaubatz (2.11.99).

Density of ZR4 : 6.57 g/cm^3

Approximation: $A_{pprox} = 1.45\ e^{-0.031\ r}$

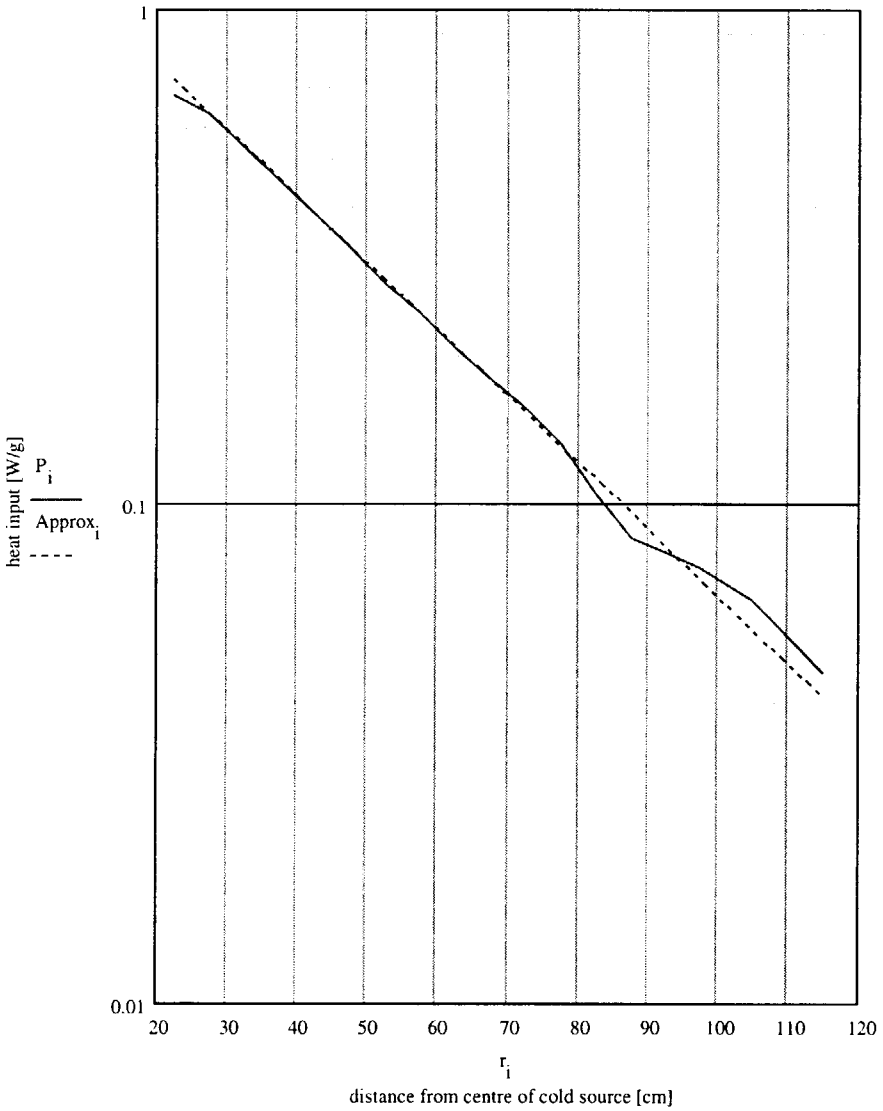

Appendix A.5

The flow - diagram and cooling circuits

The flow - diagram of the D_2 gas system and the cooling circuits are presented in Fig.A.5.1. They provide the following functionality and features.

The deuterium gas handling system

The deuterium gas system (on the left side of the flow-diagram, inside the box colored with orange background) provides preparation, filling, evacuation, and storage of the deuterium gas. The gas system satisfies the conventional requirements for a system in the nuclear-reactor environment. It is completely protected from outside by a shield of inert He gas ($1.8 \cdot 10^5$ Pa), being contained in a big vessel (in Fig.A.5.1: BB300, volume: 1.5 m^3), which is calculated to withstand a hypothetical inside explosion of a D_2-air mixture (corresponding to a static over-pressure of 13 bar).

The D_2 gas is stored in the inner vessel (BB101, 0.3 m^3) with slight under-pressure ($0.9 \cdot 10^5$ Pa). The required ortho-modification of the D_2 is prepared in the cold container (BB102, 400 cm^3) cooled by a small, separate refrigerator head (~ 10 W) at a temperature < 20 K. It can be used also for cryo-pumping.

For the exhaust of the irradiated, tritium - contaminated D_2 a system will be used, which is very similar to the approved exhaust system of the FRM II cold source. The D_2 exhaust gas will be diluted in a big vessel (BB550, ~ 1 m^3, in Fig. 14 left of BB300, the orange box) by inert nitrogen gas to less than 4% D2, the minimum concentration for ignition. Then the gas can be given to the exhaust chimney of FRM II, monitored by a tritium detector. In Appendix A.2 it is shown that the maximum amount of tritium activity, which could escape into the environment, would stay below the upper limit of the admissible per-day tritium emission (single event).

The cooling system

The specific heat input, mainly caused by γ radiation, is according to calculations by Gaubatz [Gau99] and Appendix A.4 for the different materials at the very end of the source:

Solid D_2:	~ 0.14	W/cm^3
Al6061:	~ 1.8	"
Zirkaloy:	~ 4.4	"
Liquid He:	~ 0.035	"

The heat input decreases exponentially with a characteristic length of 32.3 cm for all materials (see Appendix A.4).

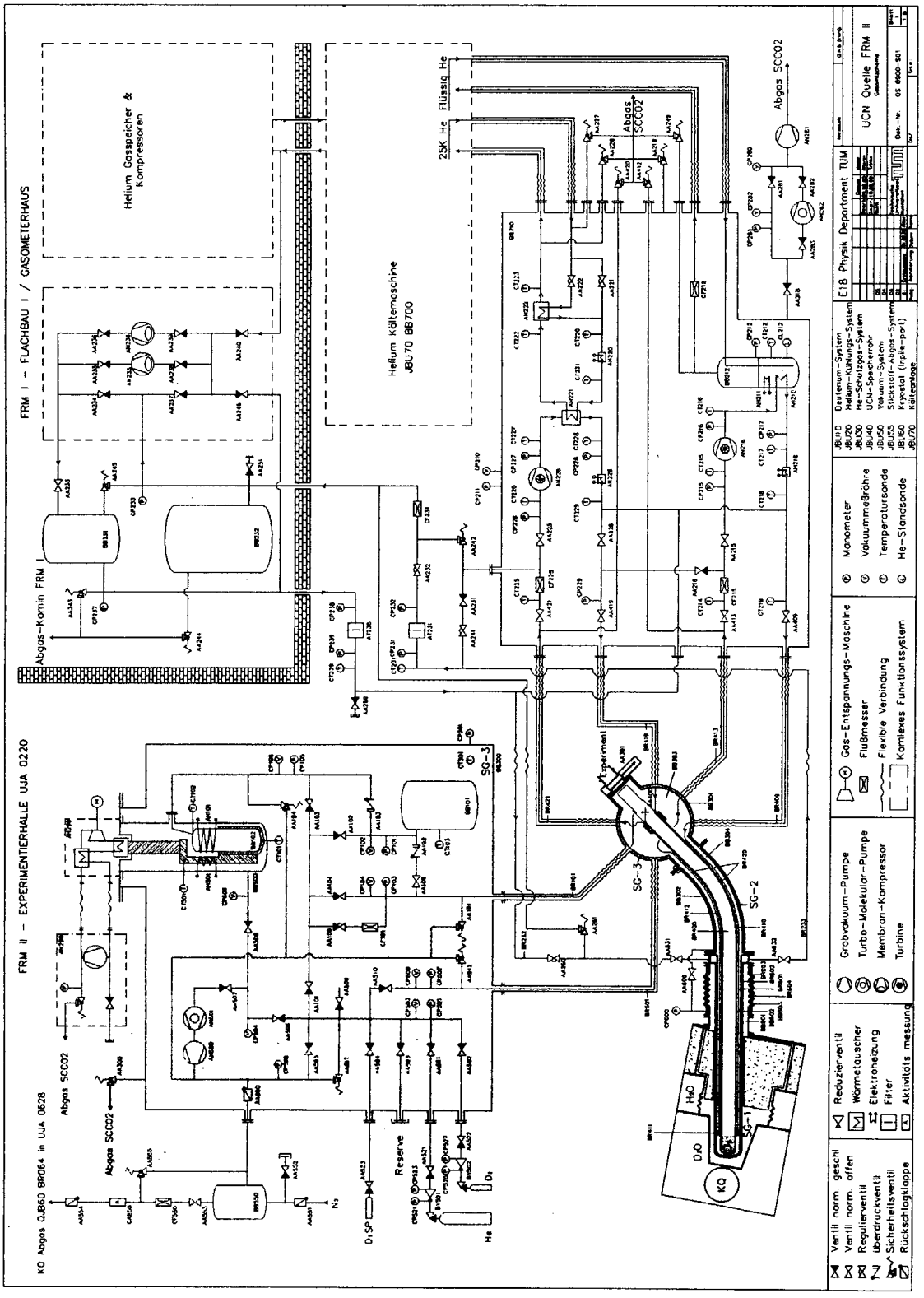

Fig. A.5.1 Flow diagram

There are three different temperature levels, at which the heat has to be cooled away. In the following list the temperature and the respective total heat load is summarized.

< 5 K level: 200 W (Converter cell with solid D_2, cooling pipes; from this: < 28 W in the D_2 converter itself)
~ 25 K level: 400 W (UCN storage tube except converter cell)
~ 300 K level: 2000 W (In-pile cryostat tube)

Correspondingly there are three He gas cooling loops operating at the different temperature levels: < 5 K, ~ 25 K, and ~ 300 K. Helium which flows in these circuits through the active zone of the nuclear reactor is contained in closed secondary systems, separated from the helium of the refrigerator primary circuit, though the estimated tritium activity from ^{3}He contamination in the ^{4}He coolant would be extremely small (see Appendix A.3). The heat exchangers for the 5 K and 25 K circuits are inside a big evacuated cryostat vessel (BB210 in Fig. 14, right-hand side, bottom).The He coolant flow in both loops is forced by mechanical, cold turbines which can overcome a pressure drop of up to 0.7 bar in the low-temperature circuits. These turbines provides very efficient cooling, resulting in a temperature difference of ~0.3 K between the walls and the coolant. An absolute reference pressure of about 3 bar is always kept with the help of a buffer reservoir (BB231, in Fig. 14 right-hand side, top), in which this value is automatically maintained from the outside by a system of membrane compressors and the large 40 m^3 storage vessel (BB232) with very clean helium. The pressure value of about 3 bar is essential to guarantee cooling by one-phase supercritical helium in the 5 K circuit, as cooling cannot be efficiently done with boiling liquid helium under the given heating conditions. Interconnections between the 5 K and 25 K loops allow cooling of both systems in series from the 25-K turbine for the standard pre-cooling procedure. When no cooling power is available the emergency room-temperature circulation can be automatically provided by the membrane compressors.

Safety aspects

In spite of a very small amount of D_2 used (40g D_2 correspond to ~200 cm^3 of wood to fire) the design takes into account all requirements concerning the safety rules at FRM II:

- Three barriers against water loss from the reactor pool
- Two barriers against deuterium loss
- Complete enclosure of deuterium by He protection gas
- At least 1 barrier withstand inner D_2 / air explosion
- Safe design with respect to specific earth quake and plane crash
- No affect on the safety of the water barriers on cooling breakdown
- No disturbance of reactor by operational failure of the UCN source
- Tritium activity below the per-day emission limit
- Helium coolant enclosed in separate secondary system

Appendix A.6

Manpower

At the Physics Department E18 of the Technical University of Munich a working group on UCN physics at the FRM II was installed under the leadership of Prof. Dr. S. Paul, presently consisting of further four senior scientists and three students. One engineer and two precision engineers are assigned to the group (all full-time). Further engeneering capacity is available from the central institutions of the Faculty of Physics, the Accelerator Laboratory of the University of Munich and the Technical University of Munich, and from FRM II.

In addition the filling of the position of a professor (C3) for UCN physics at the Pysics Department E18 is under way.

Brief biographies of the members of the UCN group

Stephan Paul, Professor (C4), Dr., head of the Physics Department E18, chairman of the research council of the Accelerator Laboratory of the University of Munich and the Technical University of Munich .....
Research: .....

Igor Altarev, Dr., senior scientist
Research: .....

Joachim Hartmann, Dr., Dr.habil., senior scientist
Research: .....

Wolfgang Schott, Dr., senior scientist
Research: experiments on neutron physics and nuclear physics, accelerator physics.

Uwe Trinks, Dr., Dr.habil., senior scientist
Research: experiments on elementary particle physics, development of neutron storage ring NESTOR, accelerator physics, development of superconduct. magnets and rf-cavities.

Collaborations

- From June 99 until June 02 we have a 'Bilateral Cooperation in Science and Technology', Reference number BRA 077/97 ENV, between the Munich UCN group and a group of scientists of the Petersburg Nuclear Physics Institute, Gatchina (head: Prof. V. Lobachev). The joint project is divided into two parts, the construction of the Mini-D2 UCN source at FRM II, and the performance of an EDM experiment at this source. For the first part the Munich group is responsible, for the second the Gatchina group.

- Sine March 99 until March 01 an INTAS cooperation is working with the title 'Investigation of a recently discovered phenomen of rare events of small energy change –heating/cooling – of UCN in traps'. In addition to the Munich group three other groups are involved: a team from the Institute Laue Langevin ILL in Grenoble with Dr.V. Nesvizhevsky as leader, a team of the Joint Institute for Nuclear Research JINR in Dubna (Laboratory of Neutron Physics) with Dr. A.V. Strelkov as leader, and a team of the Kurchatov Institute in Moscow (Laboratory of Neutron Investigations) with Dr. V.I. Morozov as leader.

- A collaboration of the Munich UCN group is being installed with the Institute for Physics (Prof. Dr. Werner Heil) and the Institute of Nuclear Chemistry (TRIGA reactor, Dr. Norbert Trautmann) of the University of Mainz, the Institute Laue-Langevin ILL in Grenoble (Dr. Peter Geltenbort and Dr. V. Nesvizhevsky) and the Joint Institute for Nuclear Research JINR in Dubna (Dr. Yu. Pokotilovski). The collaboration shall install a test facility at the pulsed TRIGA REACTOR for investigating solid D_2 and other materials (heavy methane) as UCN converters. At the TRIGA reactor thermal neutron pulses (length ~ 35 msec) with a peak flux of $5.5 \cdot 10^{14}$ n/cm^{2}s can be produced.